Laser-Induced Shape Transformation of Gold Nanoparticles below the Melting Point: The Effect of Surface Melting

Susumu Inasawa,*,† Masakazu Sugiyama,‡ and Yukio Yamaguchi†

Department of Chemical System Engineering, School of Engineering, The University of Tokyo, Hongo 7-3-1, Bunkyo-ku, Tokyo 113-8656, Japan, and Department of Electronic Engineering, School of Engineering, The University of Tokyo, Hongo 7-3-1, Bunkyo-ku, Tokyo 113-8656, Japan

Received: October 22, 2004; In Final Form: December 15, 2004

Relatively large gold nanoparticles (mean diameter of major axis 38.2 nm, mean aspect ratio 1.29) in aqueous solution were found to undergo shape transformations from ellipsoids to spheres at ca. 940 °C, which is much lower than their melting point, ca. 1060 °C. The shape transformation of gold nanoparticles induced by a single pulse of a Nd:YAG laser ($\lambda = 355$ nm, pulse width = 30 ps) was directly observed by a transmission electron microscope (TEM). Analysis of the experimental data showed that the threshold energy for photothermally induced shape transformation was on the order of 40 fJ for a particle, which is smaller than the energy, 67 fJ, required for its complete melting. Estimations based on the heat balance and surface melting model revealed that the temperature which particles reach after a single laser pulse was about 940 °C, with the thickness of the liquid layer on the surface of the solid core being 1.4 nm. We also examined thermally induced shape transformation of gold nanoparticles on Si substrates; above 950 °C they changed their shapes to spheres, which supported our estimation. Due to the surface melting of particles, their shape transformation occurs at a temperature much lower than their melting point.

Introduction

Because of their unique properties and potential applications, nanosized gold particles have received much attention. Some kinds of applications, such as biolabeling,[1] catalysts,[2,3] nonlinear optical devices,[4] optical recording media,[5] and holographic gratings,[6] have been examined; the results lead us to expect nanosized gold particles have a great future as a new material. Because the physical and chemical properties of nanosized particles depend on their size and shape, fundamental studies of gold nanoparticles are of great interest, for instance, size and shape effects on melting point,[7] optical properties[8,9] and ultrafast energy relaxation dynamics of gold nanoparticles.[9−13] It is also known that gold nanoparticles interact with visible light due to their distinct surface plasmon resonance (SPR) and interband transition (5d → 6sp).[8] Therefore intense pulsed laser light can induce size reduction,[14−30] enlargement,[18,31] and morphological changes[14,31−35] of gold nanoparticles; as well, continuous laser light induces their coagulation.[36] Photon energy absorbed by electrons heats particles due to electron−phonon scattering that occurs in a few picoseconds,[9−13] and so their temperature increases. While the extent of the temperature increase depends on the irradiated laser fluence[9,14] and the absorption coefficient at the laser wavelength,[35] it also depends on the pulse width of the laser light, since the time constant of heat dissipation from particles to surrounding solvent is on the order of 100 ps.[12] Pulsed-laser-induced morphological changes of gold nanoparticles are caused by a photothermal process.[35] Since the melting point of gold particles drastically decreases only when particle diameter is smaller than 5 nm,[7] for particles larger than 10 nm these changes are thought to occur near the bulk melting point.[14,31,35] It has been considered that the photon energy that induces the complete melting of particles is required for their morphological change to spheres.[14,31,35]

It has however been reported that the surface melting phenomenon has been observed in small metal crystals below their melting point.[37−44] A liquid layer on the rigid metal core was observed directly by dark-field electron microscopy,[37] and the thickness of the liquid layer was 20 nm for lead nanoparticles (100 nm diameter) in SiO matrix.[37] The curvature effect and less interface energy between the liquid and matrix than that between solid and matrix enhanced surface melting.[38,45,46] Further, shape transformation below the melting point of gold nanorods consisting of 10^3-10^4 atoms was clearly observed in computational simulations by Wang et al.[47] In the study of the thermally induced structural transition of gold nanoparticles by Koga and co-workers, the shape transformation of gold nanoparticles with decahedral morphology below the melting point was observed.[48] Taking these findings into account, we can expect that the shape transformation of gold nanoparticles occurs below their melting point due to surface melting of particles. Qualitatively, it would be safe to say that the temperature at which the shape transformation of particles occurs decreases with the decrease in their size, but quantitative values such as the thickness of the liquid layer and the temperature at which the shape transformation of particles can occur are still unknown.

In this paper, we report (1) the threshold energy for shape transformation of a gold nanoparticle and (2) the calculated results of the particle temperature at which shape transformation occurs and the thickness of the liquid layer, based on both heat balance and a surface melting model.[38]

The threshold energy for melting of a gold nanorod has been measured by Link et al.[35] They proposed a clear-cut way to determine the melting energy of a gold nanorod based on the absorbance change at 810 nm, corresponding to longitudinal

* Author to whom correspondence should be addressed. E-mail: inasawa@chemsys.t.u-tokyo.ac.jp.
† Department of Chemical System Engineering.
‡ Department of Electronic Engineering.

10.1021/jp045167j CCC: $30.25
Published on Web 02/05/2005

SPR,[35] but the obtained threshold energy was about 4 times larger than the value required to induce the complete melting of a nanorod.[35] Uncertainties such as the concentration of gold atoms and the wide distribution of the sizes of gold nanorods would be some of the reasons for the large threshold energy obtained in their experiments.[35] More precise experiments to determine the threshold energy for melting a gold nanoparticle in aqueous solution are needed. Our experiments used a third harmonic Nd:YAG pulsed laser ($\lambda = 355$ nm) corresponding to the interband transition of gold.[8] The absorbance of particles at 355 nm is mostly independent of their shape and size.[25] We observed shape changes of gold nanoparticles before and after a single-pulse laser heating by transmission electron microscope (TEM). The threshold energy for the shape transformation obtained by our experiments was used to calculate the particle temperature based on heat balance and the surface melting model.[38] From our experiments and calculations, it was found that the threshold energy for the shape transformation is 45 fJ per one nanoparticle, which is smaller than the required energy, 67 fJ per one nanoparticle, for complete melting. On the basis of the diameters larger than 30 nm in our study, the decrease in the melting point, which is reported to appear for a diameter as small as 5 nm,[7] is not expected. However, our calculations suggested that the shape transformation to a sphere would occur at ca. 940 °C, which is lower by more than 100 °C than the melting point for bulk. We also examined the shape transformation of gold nanoparticles on Si substrates by heating the substrates; shape transformation of gold nanoparticles below their melting point was again observed, supporting our calculations. Finally, differences between nanodots and nanorods in their shape transformations to spheres and the structure of gold nanoparticles before and after the shape transformation are discussed based on the comparison with previous works.[35,48]

Experimental Section

Gold nanoparticles were prepared by chemical reduction in aqueous solution.[49] The stock solution was made by dissolving 1 g of yellow solid of $HAuCl_4 \cdot 4H_2O$ (Wako Chemical, 99.9%) in 10 mL of purified water. A 50 mL aliquot of 0.12 mM $AuCl_4^-$ ion aqueous solution prepared by diluting the stock solution 2000 times with purified water was heated, and 180 μL of 0.1 M citric acid (Wako Chemical) aqueous solution was added at the boiling stage with vigorous stirring. The solution soon turned a wine-red color that indicated the production of gold nanoparticles. Through the use of this method, all $AuCl_4^-$ ions were reduced to gold nanoparticles. The prepared gold nanoparticles were ellipsoidal-shaped, their mean diameter at their major axis was 38.2 nm, and the mean aspect ratio was 1.29. This aqueous solution was stable for more than 1 month in a refrigerator. The solution was further diluted 4 times with purified water just before the laser irradiation experiments. The final aqueous solution of gold nanoparticles used for all experiments was 0.03 mM in atomic concentration.

A third harmonic Nd:YAG laser (EKSPLA, PL2143B) ($\lambda = 355$ nm, pulse width = 30 ps) was used for laser irradiation of the aqueous solution of gold nanoparticles. A 0.7 mL aliquot of the aqueous solution of gold nanoparticles was introduced into a rectangular quartz cell ($10 \times 10 \times 45$ mm^3, optical path 10 mm). Because we did not use any optical lenses to focus or expand the laser light, the spot size of the laser was about 9 mm in diameter. A single-pulse laser irradiation to the solution was carried out using the equipment in single-shot mode. Because of the distribution of laser intensity inside the spot, after single-pulse laser irradiation the solution in the quartz cell was carefully stirred to make it homogeneous. Irradiated laser energy was measured by a power meter (Scientech, model 362). Laser energies were also measured before and after laser light passed into a quartz cell. The absorption of laser light by an aqueous solution of gold nanoparticles was in accordance with the Lambert−Beer law. Intensity distribution inside the laser spot was determined by measuring the laser energy corresponding to each spot size, which was changed with an aperture holder (Suruga Koki, F74-3N). Absorption spectra were recorded before and after single-pulse laser irradiation, using a multichannel detector (Hamamatsu, PMA-11) and D_2 and W lamp (Hamamatsu, L7893).

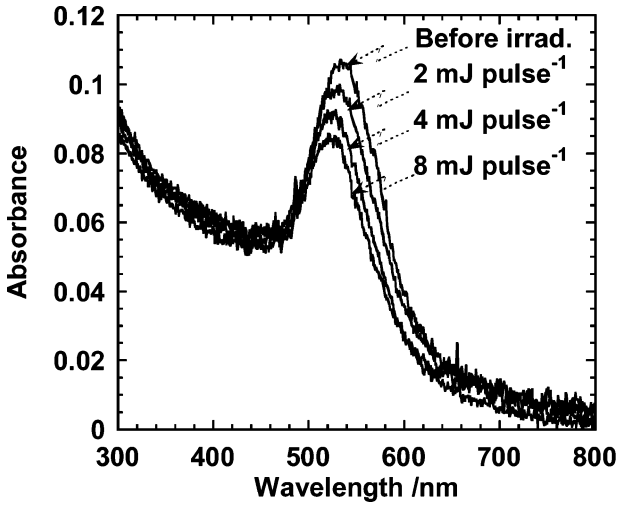

Figure 1. Absorption spectra recorded before and after single-pulse laser heating with various laser energies of 2, 4, and 8 mJ pulse^{-1}. Spectral changes are clearly observed.

For direct observation of gold nanoparticles, we used TEM (JEOL, JEM-2010) operating at 200 kV. TEM images were recorded by a CCD camera (Gatan, model 794). Samples for TEM observation were prepared by dropping 0.75 μL of the aqueous solution of gold nanoparticles onto a carbon-coated copper TEM grid and letting it dry completely. More than 450 gold nanoparticles were observed to obtain the distributions of their size and aspect ratio.

We also examined the shape transformation of gold nanoparticles on Si substrate. A 3 μL aliquot of the aqueous solution of gold nanoparticles was dropped on a Si substrate and dried at room temperature. Substrates were heated from 400 to 1074 °C in a muffle furnace (KDF, S-60). The temperature of each substrate was directly measured by a thermocouple. In each experiment, heating time was 10 min, and the desired temperature was maintained for 3 min, followed by cooling to room temperature. Before each experiment, Si substrates were immersed in a chromic acid mixture for more than 24 h and carefully washed with purified water. Nanoparticles on Si substrates were directly observed by a field-emission scanning electron microscope (FE-SEM, Hitachi, S-900). Over 200 particles were observed to obtain the mean aspect ratio of the particles. The number of particles observed by FE-SEM was relatively small, but because substrates (and also nanoparticles) are uniformly heated in a muffle furnace, we consider that shape changes of gold nanoparticles on Si substrates can be observed with these numbers of gold particles.

Results and Discussion

3.1. Observation of Shape Transformation by Laser Heating. Figure 1 shows the absorption spectra of gold

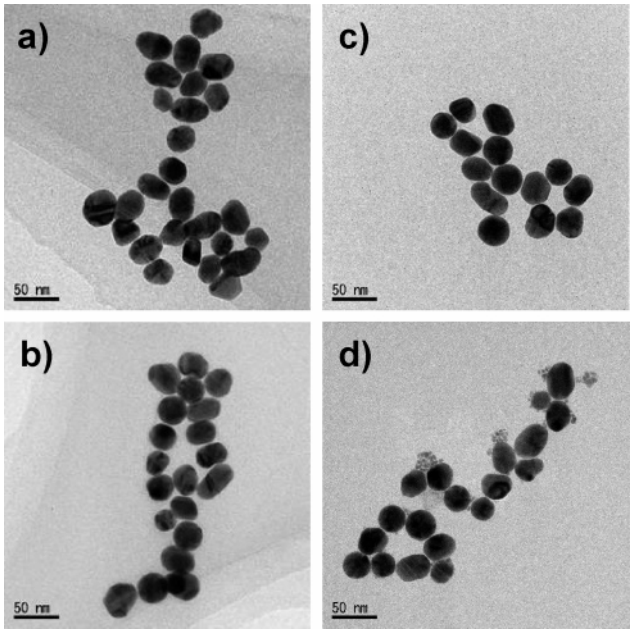

Figure 2. TEM images of gold nanoparticles (a) before heating and (b, c, and d) after single-pulse laser heating with laser energies of 2, 4, and 8 mJ pulse^{-1}, respectively.

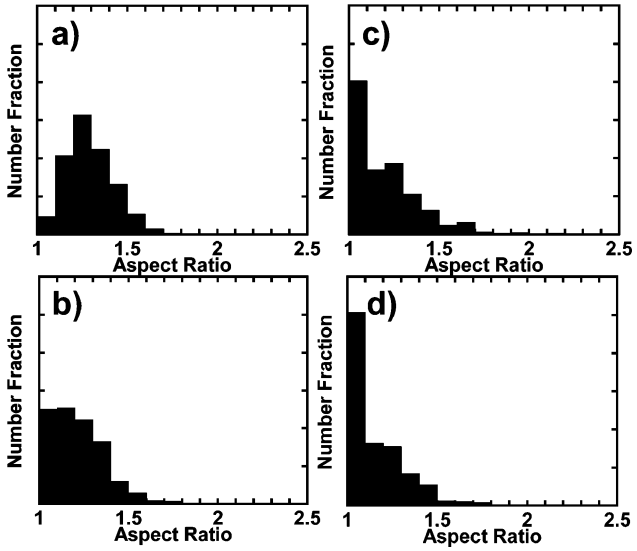

Figure 3. Distributions of the aspect ratio of gold nanoparticles obtained by TEM images (a) before and (b, c, and d) after single-pulse laser heating with laser energies of 2, 4, and 8 mJ pulse^{-1}, respectively.

nanoparticles in aqueous solutions before and after single-pulse laser heating. Laser energies measured by the power meter for each experiment are also shown. Apparent spectral changes are observed. Since the SPR of gold nanoparticles depends on their size and shape,[8,9,14,21] these changes also indicate changes of shape or size of gold nanoparticles. From Figure 1, we can expect larger changes in their size or shape with 8 mJ pulse^{-1} than with 2 mJ pulse^{-1}. Electron micrograph images for each sample taken by TEM are shown in Figure 2. Before irradiation, gold nanoparticles are mainly in ellipsoidal shape, and some have sharp edges (Figure 2a). After laser heating by a single pulse, the number of particles that have sharp edges and an ellipsoidal form decreases, and in contrast, the number of spherical particles increases with the increase in laser energy (Figure 2, parts b−d). The shape transformation of gold nanoparticles by single-pulse laser irradiation was thus confirmed. Further, we can see particles smaller than 10 nm in diameter in Figure 2d). These smaller gold nanoparticles are considered to have been produced by laser-induced size reduction.[13] The TEM images in Figure 2 suggest that the spectral change with the laser energy of 8 mJ pulse^{-1} in Figure 1 can be ascribed to the shape transformation to a sphere and the size reduction of the gold nanoparticles. As gold nanorods show an absorption spectrum with two peaks, one is at ca. 530 nm (the transverse surface plasmon bands) and the other is at ca. 800 nm (the longitudinal ones),[32−35] initial particles in ellipsoidal shapes with the aspect ratio of ca. 1.3 are also considered to show the transverse and longitudinal absorption. But because of the low aspect ratio, it is considered that those two peaks are not separated, and they overlap with each other as shown in Figure 1. Therefore the absorption peak in Figure 1 consists of two absorption peaks; one is at shorter wavelength due to transverse mode, and the other is at longer wavelength due to longitudinal mode. If the shape transformation to spheres occurs, then the longitudinal absorption decreases since the length of particles decreases, and the peak position of absorption due to the SPR of gold nanoparticles shifts to a shorter wavelength. Such blue shifts of absorption peaks are observed in Figure 1. Furthermore, because the absorption coefficient for the longitudinal mode is larger than the value for the transverse one,[32−35] the intensity of absorption also decreases with the decrease in the number of particles in ellipsoidal shapes as shown in Figure 1. As shown in Figure 2, larger laser energy led to a further decrease in ellipsoidal particles, leading to a further blue shift and smaller absorption. Size reduction phenomena can also account for these spectral changes for the laser energy of 8 mJ pulse^{-1}.

The shape transformation of gold nanoparticles is clearly shown in Figure 3, where particles smaller than a diameter of 10 nm were not counted because these smaller particles were produced by the laser-induced size reduction of the initial particles, and here we focused on the shape transformation of the initial particles to spheres. With an increase of irradiated laser energy, the number of spherical particles also increases. Here, we define a spherical particle as one whose aspect ratio is smaller than 1.1.

3.2. Threshold Energy for Shape Transformation. Here we calculate the threshold energy of a pulsed laser for shape transformation of gold nanoparticles in our system. In Figure 4, the number fractions of spherical particles are plotted with respect to irradiated laser energy. With an increase of laser energy, the number fractions of spherical particles increases, but the increase becomes gradual for more intense laser energy. In the following analysis, we assume that shape transformation occurs while the number of the particles is unchanged. The laser-induced size reduction, which occurs at a larger laser energy, hardly changes the total number of particles that are larger than 10 nm, as described in Appendix A.

On the basis of the results shown in Figure 4, we calculated the threshold energy of the pulsed laser for the shape transformation of gold nanoparticles. Our measurements showed that the intensity distribution inside the laser spot well agreed with Gaussian values, with a specific radius a (0.223 cm), as

$$I = I_0 \, e^{-r^2/a^2} \tag{1}$$

where r is the distance from the center of the laser spot, I_0 is the maximum laser energy per unit area, and I is the laser energy

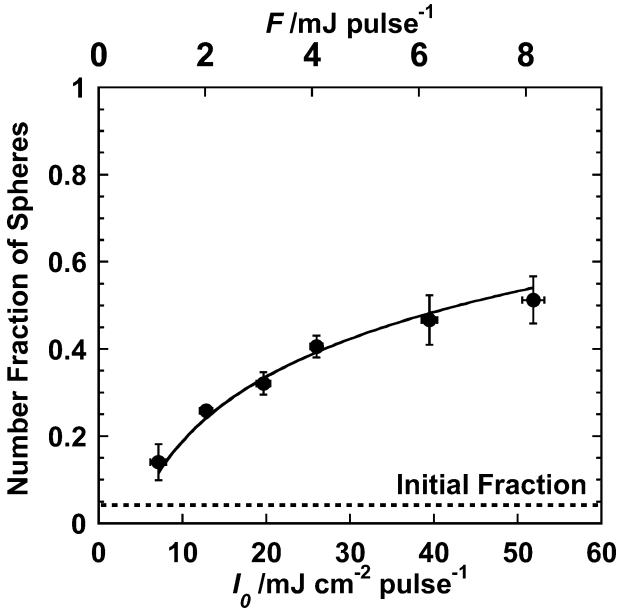

Figure 4. Dependence of the number fraction of spherical particles on irradiated laser energy. Both measured laser energy F and converted laser energy I_0 are shown. Spherical particles mean particles with an aspect ratio smaller than 1.1 in Figure 3. The solid line is the fitting result based on eq 3 with a single fitting parameter $I_{th} = 5.6 \pm 0.9$ mJ cm^{-2} pulse^{-1}.

per unit area at the distance r. I_0 is related to the experimentally measured laser energy F as

$$F = \pi a^2 I_0 \tag{2}$$

Provided that all of the gold nanoparticles heated by a single laser pulse with energy larger than the threshold for shape transformation turn into spherical ones, we can describe the number fraction of spherical particles in aqueous solution after laser heating as

$$\eta = (1 - \eta_0)\frac{V}{V_0} + \eta_0 \tag{3}$$

where η_0 (0.046) and η are the numbers of spherical particles before and after laser heating, respectively, V is the volume that is irradiated by a single pulse with energy larger than the threshold, and V_0 is the total volume of the aqueous solution in a quartz cell (0.7 cm^3). V is analytically obtained by using the threshold laser energy for shape transformation, I_{th} (Appendix B), as

$$V = -\pi a^2\left(\ln\left(\frac{I_{th}}{I_0}\right) + \frac{2.303\epsilon C_{Au}}{2}\right) \tag{4}$$

where ϵ is the absorption coefficient of gold atoms at 355 nm and C_{Au} is the concentration of gold atoms. The last term on the right side in eq 4 corresponds to the attenuation of laser light in a sample solution. It was derived by considering the Lambert−Beer law in a sample solution. (Appendix B)

We can fit eq 3 to the experimental data shown in Figure 4 with I_{th} as a single fitting parameter. Figure 4 shows excellent agreement between eq 3 and our experimental data, and we obtained the threshold energy of the laser as $I_{th} = 5.6 \pm 0.9$ mJ cm^{-2} pulse^{-1} with $\epsilon C_{Au} = 0.065$ cm^{-1} at 355 nm (Figure 1).

On the basis of the assumption that the shape transformation occurs by a photothermal process, we calculated particle

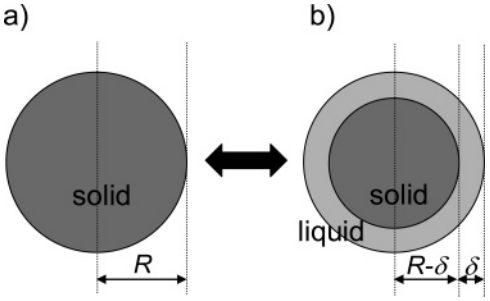

Figure 5. Schemes for surface melting showing a (a) solid particle and (b) liquid layer with a thickness of δ on the surface of the solid core.

temperature after laser heating with this threshold value. It was suggested that the photoinduced ionization of gold nanorods can occur by the femtosecond laser pulses of extremely high energy.[28] However, it was also suggested that the shape transformation of gold nanorods by femtosecond laser pulses with smaller energy corresponding to the melting point of nanorods occurs by a photothermal process.[35] Considering that we used picosecond laser pulses with laser energy roughly corresponding to the melting point of the particles, we can exclude the possibility of photoinduced ionization of gold nanoparticles.

Because the time constant for heat dissipation from particles to surrounding water is on the order of 100 ps[12] and the pulse width of our laser is 30 ps, heat dissipation from particles is negligible. The temperature of particles after a single-pulse laser heating, T_p, is calculated as, assuming room temperature of 20 °C,

$$T_p = \frac{I_{th}(1 - 10^{-\epsilon C_{Au} l_0})}{C_p C_{Au} l_0} + 20 \tag{5}$$

where C_p is the specific heat of bulk gold and l_0 is the path length. T_p is estimated to be 1040 °C, using the following values: the path length $l_0 = 1$ cm, $C_p = 25.4$ J mol, $C_{Au} = 3 \times 10^{-8}$ mol cm^{-3}. The estimated value based on eq 5 corresponds to the maximum temperature of a particle because we assumed all absorbed photon energy turned into thermal energy.

Because the melting point of gold nanoparticles used in our experiments is almost the same as the bulk value[7] (1064 °C) and the enthalpy of fusion (12.7 kJ mol^{-1}) is also required for melting, our estimation shows that the obtained value of I_{th} is not sufficient to induce significant melting of the particles. The assumption of a single phase in a particle, uniform temperature, and the melting point of bulk gold led to the conclusion that the shape transformation occurred at a laser energy that would be insufficient to melt the particle. However, shape transformation without melting is not easy to accept. We consider that we can avoid this contradiction by assuming surface melting, as discussed below.

3.3. Surface Melting of Gold Nanoparticles. A phenomenological model for surface melting was proposed to consider the curvature effects of particles.[38] On the basis of this model, we estimated the particle temperature at which the shape transformation can occur. The free energies of a solid particle with radius R (Figure 5a), G_s, and a solid particle with liquid layer on its surface (Figure 5b), G_{sl}, are

$$G_s = n_0 \mu_s + 4\pi R^2 \gamma_{sv} \tag{6}$$

and

$$G_{sl} = (n_0 - n_s)\mu_l + n_s\mu_s + 4\pi R^2\gamma_{lv} + 4\pi(R-\delta)^2\gamma_{sl} + 4\pi R^2 S \exp\left(-\frac{\delta}{\xi}\right) \quad (7)$$

where n is the numbers of moles, μ is the chemical potential, and γ is interface energy. Subscripts s, l, and v stand for solid, liquid, and vapor, respectively. δ is the thickness of the liquid layer on the solid core. The last term on the right side in eq 7 is introduced to describe the short-range interaction between two interfaces,[38,51] and ξ is the correlation length. In eq 7, S is written as[38,51]

$$S = \gamma_{sv} - \left(\gamma_{lv} + \left(\frac{R-\delta}{R}\right)^2\gamma_{sl}\right) \quad (8)$$

Minimization of $G_{sl} - G_s$ gives

$$\frac{\Delta T}{T_m} = \frac{2\gamma_{sl}}{\rho\Delta H_f(R-\delta)}\left(1 - \exp\left(-\frac{\delta}{\xi}\right)\right) + \frac{SR^2}{\rho\Delta H_f\xi(R-\delta)^2}\exp\left(-\frac{\delta}{\xi}\right) \quad (9)$$

where T_m is the melting point ($\Delta T = T_m - T$), ρ is the density of materials in liquid phase, and ΔH_f is the enthalpy of fusion. We used the assumptions that the densities of the liquids and solids are equal and $\mu_l - \mu_s$ is approximated by $\Delta H_f \Delta T/T_m$.[38,51] In calculating eq 9, we have to determine the value of the correlation length ξ. For Pb, the correlation length was experimentally determined to be $\xi_{Pb} = 0.63$ nm,[40] and for Cu it was determined to be $\xi_{Cu} = 0.43$ nm by molecular dynamics simulations.[52] The lattice constant of Pb is 0.49505 nm, and for Cu it is 0.36150 nm.[50] The ratio between correlation lengths and each lattice constant are 1.27 for Pb and 1.18 for Cu. By analogy, the correlation length of gold is considered to be 0.5 nm, because the lattice constant of gold is 0.40786 nm[50] and the values of the lattice constant multiplied by 1.2 and 1.3 are 0.49 and 0.53 nm, respectively. Therefore, we accept 0.5 nm as the correlation length of gold.

We also calculated particle temperatures based on heat balance. We can write the particle temperature T °C as

$$T = \frac{I_{th}(1 - 10^{-\epsilon C_{Au} l_0}) - \Delta H_f(1-\alpha)C_{Au}}{C_p C_{Au} l_0} + 20 \quad (10)$$

where

$$\alpha = \frac{(b_l - \delta)(b_s - \delta)^2}{b_l b_s^2} \quad (11)$$

with the assumptions that (1) particles have a uniform liquid layer with thickness δ on the surface of the solid core at their shape transformation stage, (2) the volume of a standard particle used in our experiments is $4\pi b_l b_s^2/3$ (b_l and b_s are the radii in the major and minor axis of a particle, respectively), and (3) a liquid layer is produced by absorbing the enthalpy of fusion.

By solving eqs 9 and 10, we can obtain the thickness of the liquid layer δ and the particle temperature T, using the values $\Delta H_f = 6.46 \times 10^4$ J kg,[50] $\rho = 1.73 \times 10^3$ kg m^{-3},[50] $T_m = 1337.15$ K,[50] $\gamma_{sv} = 1.7-2.0$ N m^{-1},[53] $\gamma_{lv} = 1.135$ N m^{-1},[7,54] $\gamma_{sl} = 0.270$ N m^{-1},[7,54] $b_l = 19.1$ nm, $b_s = 14.8$ nm, and $R =$ 16.8 nm, which is the square root of $b_l b_s$. The differences in the free energies, $G_{sl} - G_s$, for various temperatures are shown in Figure 6. The steady-state value of δ is obtained from the minimal energy point for each temperature. Because the phase transition of gold nanoparticles is considered to occur before the shape transformation and the time constant for shape transformation of gold nanorods due to complete melting is ca. 30 ps,[33] the time constant for the phase transition from solid to liquid is faster than the pulse width of 30 ps. Therefore, we consider that the steady-state value of δ corresponds to the thickness of the liquid layer on the solid surface just after laser heating.

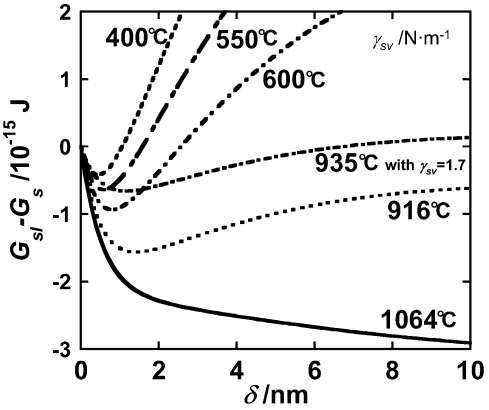

Figure 6. Calculation results of the difference of free energies, $G_{sl} - G_s$, with various temperatures. Note that $\gamma_{sv} = 1.7$ N m^{-1} is used only for 935 °C, $\gamma_{sv} = 2.0$ N m^{-1} for others. (γ_{sv} is the interfacial energy between solid and vapor.)

At 1064 °C, $G_{sl} - G_s$ decreases monotonically with δ, meaning the melting of a whole particle. Equations 9 and 10 are satisfied by $T = 916$ °C, $\delta = 1.4$ nm for $\gamma_{sv} = 2.0$ N m^{-1}, and $T = 935$ °C, $\delta = 1.2$ nm for $\gamma_{sv} = 1.7$ N m^{-1}. As already described, we defined a sphere as those particles having an aspect ratio smaller than 1.1; therefore, when ellipsoid particles of diameter 38.2 nm in their major axis and an aspect ratio of 1.29 turn into spherical ones with the aspect ratio of 1.1, the required thickness of the liquid layer is calculated to be at least 1.5 nm,[55] which roughly agrees with calculation results based on eqs 9 and 10. These results support the shape transformation of gold nanoparticles due to surface melting far below their melting point. Note that considering the error in the threshold laser energy the estimated temperature includes about 10% error. The correlation length ξ also has uncertainty, but the value is considered to be in the range of 0.4−0.6 nm, as described above. The variation of the correlation length in such range gives the estimated temperature about 2% error.

The temperatures in the discussion above are based on estimations; therefore, we observed the shape transformation of gold nanoparticles under the condition where the temperature is precisely measured. Images of particles on Si substrates by FE-SEM are shown in Figure 7. Gold particles are taken as being the white parts. Below 550 °C, ellipsoid particles were observed, while at 950 °C particles were nearly of a spherical shape. At 850 °C, most particles changed their shape to spheres while some remained ellipsoidal-shaped. In Figure 8, the mean aspect ratio of the gold particles was plotted to each substrate temperature. Because of the interaction between particles and the substrate surface, such as friction or adsorption, the mean aspect ratio does not decrease to 1 even above the melting point. The mean aspect ratio of the particles at 950 °C is the same as

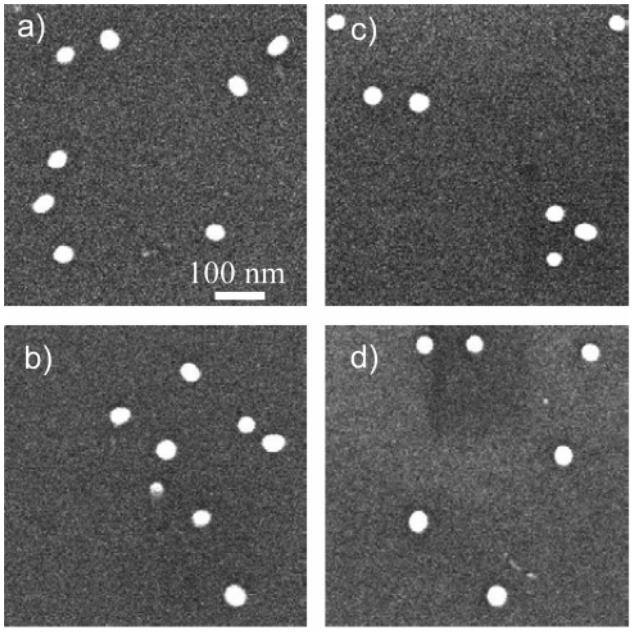

Figure 7. FE-SEM images of gold nanoparticles on Si substrates (a) before and (b, c, and d) after 3 min maintenance at 550, 850, and 950 °C, respectively.

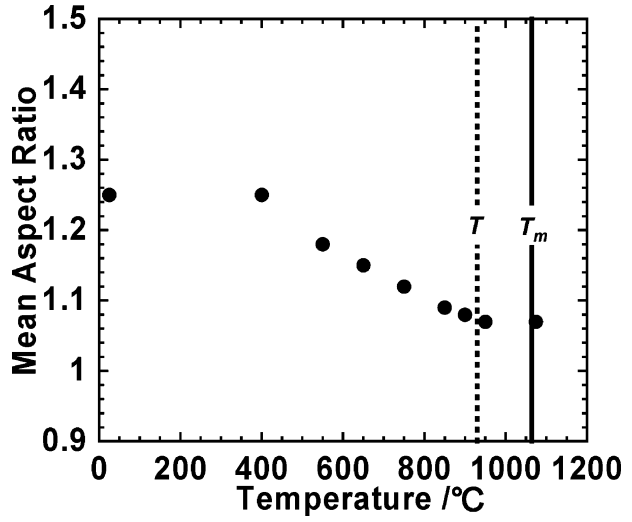

Figure 8. Dependence of the mean aspect ratio of gold nanoparticles on the substrate temperature. *T* stands for the calculated temperature based on eqs 9 and 10, and T_m is the melting point of bulk gold.

the value at 1074 °C, meaning that the shape transformation of gold nanoparticles occurs far below their melting point.

If significant melting of gold particles would be required to cause the shape transformation, then a sudden decrease of the mean aspect ratio would be expected near the melting point in Figure 8. But a gradual decrease of the aspect ratio is observed in Figure 8; surface melting of particles also explains this gradual decrease. A thin liquid layer on the solid core is expected to be formed even far below the melting point, as shown in Figure 6. After the formation of the liquid layer, the surface of the particle becomes rounded off due to the surface tension of the liquid. Because the degree of the shape transformation depends on the thickness of the liquid layer and the thickness of the liquid layer depends on temperature, the mean aspect ratio of gold nanoparticles gradually decreases. A wide distribution of gold nanoparticle sizes can also induce a gradual decrease of the mean aspect ratio.

3.4 Comparison with Previous Work. The threshold energy for the shape transformation of a particle, $I_{th,p}$, is calculated as

$$I_{th,p} \approx \frac{I_{th}(1 - 10^{-\epsilon C_{Au} l_0})}{C_{Au} l_0} \frac{4\pi}{3} b_l b_s^2 \rho_s \qquad (12)$$

where ρ_s is the density of gold in the solid phase (9.8×10^4 mol m^{-3}). From eq 12, $I_{th,p}$ is obtained as 45 fJ, which is 4.4×10^{-20} J per one atom. If the complete melting of a particle is considered, then the required energy is estimated as 67 fJ, which is 6.5×10^{-20} J per one atom. Link et al. made a spectroscopic determination of the threshold energy to transform a gold nanorod with an aspect ratio of 4 to a sphere as 65 fJ, while the complete melting of a gold nanorod required 16 fJ.[35] Their nanorod consisted of roughly 246 700 atoms. Therefore, the threshold energy for the shape transformation is 2.6×10^{-19} J per one atom, which is larger than the energy, 6.5×10^{-20} J per one atom, required for complete melting. Considering the potential experimental errors they proposed, their result is seemingly contradictory to our findings that the shape transformation proceeds at a lower energy than that required for complete melting. However, it can be concluded that the nanorod they used required its complete melting. A simple calculation based on ref 55 suggests that the thickness of the liquid layer should be at least 9.0 nm for shape transformation of a gold nanorod (aspect ratio 4, width 11 nm, length 44 nm)[35] to a sphere with an aspect ratio of 1.1. Considering that about 40% of the length of a nanorod should melt and eq 9 predicts that surface melting can occur only with a thickness of the liquid layer thinner than 2.2 nm, such kinds of surface melting with a thick liquid layer is thought to be impossible. That is that, unlike with our particles, the shape transformation of a nanorod to a sphere would require its complete melting.

The structural transition of gold nanoparticles before and after the shape transformation should be also discussed. Koga et al. reported the structural transition of gold nanoparticles in the range of 3−18 nm.[48] In their report, the structural transition from icosahedral (Ih) to decahedral (Dh) just below the melting point and the structural transition from Dh to fcc above the melting point[48] were observed. If the shape transformation of gold nanoparticles is induced by the structural transition, then our discussion contradicts the experimental results by Koga et al.[48] However, in the same paper, they also reported the shape transformation to spheres far below their melting point by ca. 100 K without their structural transition,[48] and hence the shape transformation of gold nanoparticles does not necessarily require the structural transition. Although we have not identified the structure of the particles, it is probable that the shape transformation of gold nanoparticles in our experiment occurs with their structures hardly changed far below the melting point of the particles.

Conclusion

We demonstrated that the shape transformation of relatively large gold nanoparticles (mean diameter 38.2 nm, aspect ratio 1.29) occurred below their melting point. The shape transformation is caused by the surface melting of particles. Our calculations based on our laser heating experiment and the surface melting model reveals that shape transformation can occur at ca. 940 °C, which is lower by 100 °C than the melting point, with the thickness of the liquid layer being 1.4 nm. The shape transformation of particles on Si substrates also shows that surface melting plays an important role in their shape transformation and supports our calculation results. Unlike with our

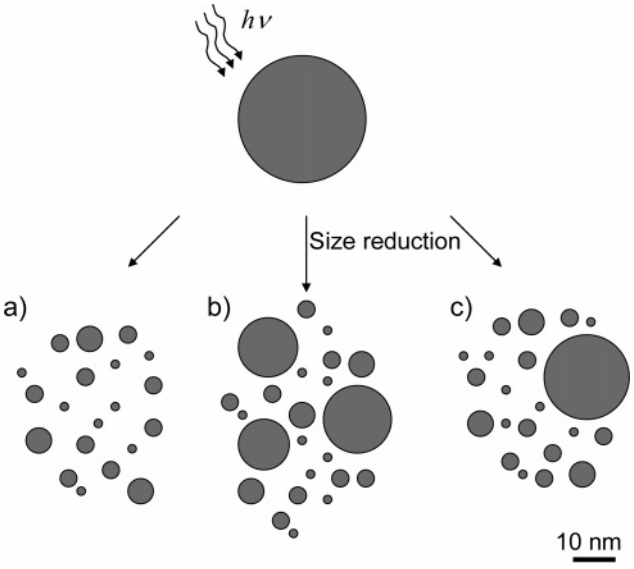

Figure A1. Schemes for laser-induced size reduction of gold nanoparticles. Three possibilities are considered. An initial particle turns into (a) particles smaller than 10 nm in diameter, (b) several particles larger than 10 nm and other particles smaller than 10 nm, or (c) one particle larger than 10 nm and other particles smaller than 10 nm. For the effect of the size reduction on the total number of particles, see the text.

particles, gold nanorods, because of their large aspect ratio, would require their complete melting for shape transformation to a sphere.

Acknowledgment. This work was supported by the "Nanotechnology Materials Programs—Nanotechnology Particle Project" of the New Energy and Industrial Technology Development Organization (NEDO) based on funds provided by the Ministry of Economy, Trade and Industry, Japan (METI). We also thank the High Voltage Electron Microscope Laboratory, School of Engineering, The University of Tokyo, for their technical support for TEM.

Appendix A

Since we also observed laser-induced size reduction of gold nanoparticles in Figure 2d and the number of particles increased due to the size reduction, it is considered that size reduction affects the number fraction of spherical particles. As described in the text, because we counted particles larger than a diameter of 10 nm, three types of size reduction can be considered, as shown in Figure A1. An initial particle turns into (a) particles with a diameter smaller than 10 nm, (b) some particles larger than 10 nm and other particles smaller than 10 nm, or (c) one particle larger than 10 nm and particles smaller than 10 nm. Total numbers of particles larger than 10 nm decrease in the case of Figure A1, part a, and increase in case of Figure A1, part b. In the case of Figure A1, part c, the number is unchanged. In Figure 2d, the diameter of small particles produced by the laser-induced size reduction of initial particles is about 4 nm. For the size reduction in Figure A1, part a, an initial particle with a 38.2 nm diameter turns into about 800 particles with diameters of 4 nm. That is that many smaller particles are expected to be observed in TEM images if the size reduction in Figure A1, part a, is dominant. But as seen in Figure 2d, the number of smaller particles is not so many, meaning that the laser-induced size reduction in Figure A1, part a, is not dominant. In the case of Figure A1, part b, the number of particles larger than 10 nm is expected to increase. Figure A2

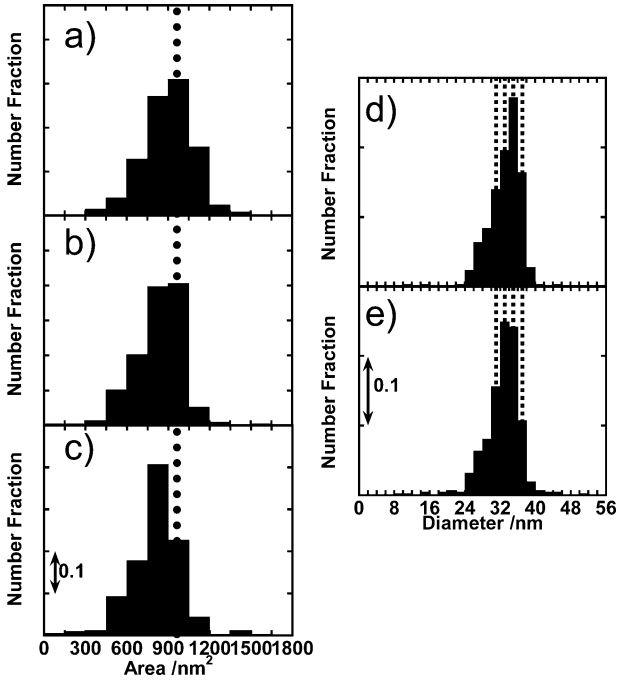

Figure A2. Area distributions (left) and size distributions (right) of gold nanoparticles (a) before laser heating and (b and c) after a single-pulse laser heating with laser energies 4 and 8 mJ pulse^{-1}, respectively. Parts d and e are size distributions after single-pulse laser heating with laser energies of 4 and 8 mJ pulse^{-1}, respectively. Note that only spherical particles are counted for parts b−e. Dotted lines provide a visual guide.

shows areas and size distributions of gold nanoparticles before and after single-pulse irradiation. The area distribution of spherical particles for the 4 mJ pulse^{-1} is nearly the same with the one for before irradiation (Figure A2, parts a and b). This means that shape transformation without a significant size reduction occurs with the laser energy of 4 mJ pulse^{-1}. For the 8 mJ pulse^{-1} in Figure A2, part c, area reduction due to the size reduction of particles is observed. As shown in Figure A2, parts d and e, which are size distributions of spherical particles after laser irradiation with energies of 4 and 8 mJ pulse^{-1}, only a slight increase in the number fraction between 30 and 34 nm is observed, while the number fractions between 34 and 38 nm decrease. The net amount of the increase in the number fraction between 30 and 34 nm roughly agrees with the net amount of decrease between 34 and 38 nm (Figure A2, parts d and e). This suggests that size reduction in Figure A2, part b, is also not dominant. Therefore, we concluded that the total number of particles larger than 10 nm is hardly affected by the size reduction of gold nanoparticles.

Appendix B

From eq 1, the threshold laser energy for the shape transformation, I_{th}, is related to the distance from the center of the laser spot, r_{th}, as

$$I_{th} = I_0 \, e^{-r_{th}^2/a^2} \tag{B1}$$

V is expressed in terms of geometrical relations as

$$V = \int_0^1 \pi r_{th}^{\,2} \, dl \tag{B2}$$

where l is the length with respect to optical path direction. Because laser light is attenuated in accordance with the

Lambert−Beer law, I_0 should be replaced with $I_0 10^{-\epsilon C_{Au} l}$ in eq B2. From eqs B1 and B2, we obtain eq 4.

References and Notes

(1) Lin, C. C.; Yeh, Y. C.; Chen, C. L.; Chen, G. F.; Chen, C. C.; Wu, Y. C. *J. Am. Chem. Soc.* **2002**, *124*, 3508.

(2) Guczi, L.; Horvath, D.; Paszti, Z.; Peto, G. *Catal. Today* **2002**, *72*, 101.

(3) Kawasaki, T.; Takai, Y.; Shimizu, R. *Appl. Phys. Lett.* **2001**, *79*, 3509.

(4) Hamakawa, Y.; Fukuta, K.; Nakamura, A.; Liz-Marzan, L. M.; Mulvaney, P. *Appl. Phys. Lett.* **2004**, *84*, 4938.

(5) Sugiyama, M.; Inasawa, S.; Koda, S.; Hirose, T.; Yonekawa, T.; Omatsu, T.; Takami, A. *Appl. Phys. Lett.* **2001**, *79*, 1528.

(6) Hirose, T.; Omatsu, T.; Sugiyama, M.; Inasawa, S.; Koda, S. *Chem. Phys. Lett.* **2004**, *390*, 166.

(7) Buffat, Ph.; Borel, J.-P. *Phys. Rev. A* **1976**, *13*, 2287.

(8) Alvarez, M. M.; Khoury, J. T.; Schaaff, T. G.; Shafigullin, M. N.; Vezmar, I.; Whetten, R. L. *J. Phys. Chem. B* **1997**, *101*, 3706.

(9) Link, S.; El-Sayed, M. A. *J. Phys. Chem. B* **1999**, *103*, 8410.

(10) Link, S.; Burda, C.; Mohamad, M. B.; Nikoobakht, B.; El-Sayed, M. A. *Phys. Rev. B* **2000**, *61*, 6086.

(11) Logunov, S. L.; Ahmadi, T. S.; El-Sayed, M. A.; Khoury, J. T.; Whetten, R. L. *J. Phys. Chem. B* **1997**, *101*, 3713.

(12) Hodak, J. H.; Martini, I.; Hartland, G. V. *J. Phys. Chem. B* **1998**, *102*, 6958.

(13) Shin, H. H.; Hwang, I. W.; Hwang, Y. N.; Kim, D.; Han, S. H.; Lee, J. S.; Cho, G. *J. Phys. Chem. B* **2003**, *107*, 4699.

(14) Takami, A.; Kurita, H.; Koda, S. *J. Phys. Chem. B* **1999**, *103*, 1226.

(15) Takami, A.; Yamada, H.; Nakano, K.; Koda, S. *Jpn. J. Appl. Phys., Part 2* **1996**, *35*, L781.

(16) Kurita, H.; Takami, A.; Koda, S. *Appl. Phys. Lett.* **1998**, *72*, 789.

(17) Kamat, P. V.; Flumiani, M.; Hartland, G. V. *J. Phys. Chem. B* **1998**, *102*, 3123.

(18) Fujiwara, H.; Yanagida, S.; Kamat, P. V. *J. Phys. Chem. B* **1999**, *103*, 2589.

(19) Inasawa, S.; Sugiyama, M.; Koda, S. *Jpn. J. Appl. Phys., Part 1* **2003**, *42*, 6705.

(20) Hirose, T.; Omatsu, T.; Sugiyama, M.; Inazawa, S.; Takami, A.; Tateda, M.; Koda, S. *Jpn. J. Appl. Phys., Part 1* **2003**, *42*, 1288.

(21) Mafune, F.; Kohno, J.; Takeda, Y.; Kondow, T.; Sawabe, H. *J. Phys. Chem. B* **2001**, *105*, 5114.

(22) Mafune, F.; Kohno, J.; Takeda, Y.; Kondow, T. *J. Phys. Chem. B* **2001**, *105*, 9050.

(23) Mafune, F.; Kohno, J.Y.; Takeda, Y.; Kondow, T. *J. Phys. Chem. B* **2002**, *106*, 7575.

(24) Mafune, F.; Kohno, J.Y.; Takeda, Y.; Kondow, T. *J. Phys. Chem. B* **2002**, *106*, 8555.

(25) Mafune, F.; Kondow, T. *Chem. Phys. Lett.* **2003**, *372*, 199.

(26) Mafune, F.; Kohno, J.; Takeda, Y.; Kondow, T. *J. Phys. Chem. B* **2003**, *107*, 12589.

(27) Link, S.; Burda, C.; Mohamed, M. B. Nikoobakht, B.; El-Sayed, M. A. *J. Phys. Chem. A* **1999**, *103*, 1165.

(28) Link, S.; Burda, C.; Nikoobakht, B.; El-Sayed, M. A. *J. Phys. Chem. B* **2000**, *104*, 6152.

(29) Francois, L.; Mostafavi, M.; Belloni, J.; Delouis, J. F.; Delaire, J.; Feneyrou, P. *J. Phys. Chem. B* **2000**, *104*, 6133.

(30) Francois, L.; Mostafavi, M.; Belloni, J.; Delaire, J. A. *Phys. Chem. Chem. Phys.* **2001**, *3*, 4965.

(31) Kawasaki, M.; Hori, M. *J. Phys. Chem. B* **2003**, *107*, 6760.

(32) Chang, S. S.; Shih, C. W.; Chen, C. D.; Lai, W. C.; Wang, C. R. C. *Langmuir* **1999**, *15*, 701.

(33) Link, S.; Burda, C.; Nikoobakht, B.; El-Sayed, M. A. *Chem. Phys. Lett.* **1999**, *315*, 12.

(34) Link, S.; Wang, Z. L.; El-Sayed, M. A. *J. Phys. Chem. B* **2000**, *104*, 7867.

(35) Link, S.; El-Sayed, M. A. *J. Chem. Phys.* **2001**, *114*, 2362.

(36) Takeuchi, Y.; Ida, T.; Kimura, K. *J. Phys. Chem. B* **1997**, *101*, 1322.

(37) Lereah, Y.; Deutscher, G.; Cheyssac, P.; Kofman, R. *Europhys. Lett.* **1990**, *12*, 709.

(38) Kofman, R.; Cheyssac, P.; Aouaj, A.; Lereah, Y.; Deutscher, G.; Ben-Devid, T.; Penisson, J. M.; Bourret, A. *Surf. Sci.* **1994**, *303*, 231.

(39) Lai, S. L.; Guo, J. Y.; Petrova, V.; Ramanath, G.; Allen, L. H. *Phys. Rev. Lett.* **1996**, *77*, 99.

(40) Pluis, B.; Taylor, T.; N.; Frenkel, D.; van der Veen, J. F. *Phys. Rev. B* **1989**, *40*, 1353.

(41) Peters, K. F.; Cohen, J. B.; Chung, Y. W. *Phys. Rev. B* **1998**, *13*, 430.

(42) Peters, K. F.; Chung, Y. W.; Cohen, J. B. *Appl. Phys. Lett.* **1997**, *71*, 2391.

(43) Wang, Z. L.; Petroski, J. M.; Green, T. C. El-Sayed, M. A. *J. Phys. Chem. B* **1998**, *102*, 6145.

(44) Mohamed, M. B.; Wang, Z. L.; El-Sayed, M. A. *J. Phys. Chem. A* **1999**, *103*, 10255.

(45) Bohr, J. *Europhys. Lett.* **1991**, *14*, 85.

(46) Lereah, Y.; Deutscher, G.; Cheyssac, P.; Kofman, R. *Europhys. Lett.* **1991**, *14*, 87.

(47) Wang, Y.; Dellago, C. *J. Phys. Chem. B* **2003**, *107*, 9214.

(48) Koga, K.; Ikeshoji, T.; Sugawara, K. *Phys. Rev. Lett.* **2004**, *92*, 115507.

(49) Kreibig, U.; Vollmer, M. *Optical Properties of Metal Clusters*; Springer: Berlin, 1995.

(50) *Handbook of Chemistry and Physics*, 83rd ed.; CRC Press: Boca Raton, FL, 2002.

(51) Brouchton, J. Q.; Gilmer, G. H. *Acta Metall.* **1983**, *31*, 845.

(52) Barnett, R. N.; Landman, U. *Phys. Rev. B* **1991**, *44*, 3226.

(53) Solliard, C.; Flueli, M. *Surf. Sci.* **1985**, *156*, 487.

(54) Smables, J. R. *Proc. R. Soc. London, Ser. A* **1971**, *324*, 339.

(55) After the shape transformation, the length of major axis of a particle b_l' should satisfy $\pi b_l^2/1.29 = \pi b_l'^2/1.1$, then $b_l' = 17.6$ nm and $b_l - b_l'$ is the minimal thickness of liquid layer for the shape transformation.